16TH EUROPEAN CONFERENCE ON EARTHQUAKE ENGINEERING THESSALONIKI 18 - 21 JUNE 2018

ANALYSIS OF THE OUTRIGGER SYSTEM WITH ROTATION INERTIA DAMPER

Ping TAN[1], Liangkun LIU[2], Haitao Ma[3], Weiming YAN[4], Fulin ZHOU[5], Shi Huan[6]

ABSTRACT

A novel damper, rotation inertia damper (RID), possessing the advantage of displacement amplification, has been employed in outrigger system for seismic mitigation. An equivalent analysis model composed of a uniform cantilever beam and an equivalent spring was proposed to simulate the RID outrigger system, by which the corresponding dynamic characteristic equation was derived by use of the numerical assembly technique. Finite-element method has been utilized to obtain its response. The results show that the pseudo-undamped natural frequency ratios and modal damping ratios of the system are significantly influenced by stiffness parameter of the exterior column, while the mass parameter of the RID has little effect on them. Furthermore, numerical simulation results for the typical earthquake records also show that RID outrigger system has excellent control performance in displacement as well as in acceleration.

Keywords: Rotation inertia damper (RID) outrigger; Seismic mitigation; Dynamic characteristics; Numerical assembly technique; Control performance

1. INTRODUCTION

Suppressing excessive vibrations of the structure and reducing them to a reasonable range is a challenge for many engineers . However, it has been known that the assumed damping for many high-rise buildings is overestimated (Satake et al. 2003; Smith and Willford, 2007), which makes it even more important to enhance the energy dissipation of the structure.

Recently, damped outrigger system has been proposed by Smith and Willford (2007) to reduce the excessive dynamic response (Willford et al., 2008). In order to explore the damping characteristics, Chen et al. (2010) assumed that the core is a cantilever beam with peripheral columns of infinite stiffness. Furthermore, semi-active control devices, MR dampers, were also adopted to replace the traditional dampers installed between peripheral columns and outriggers (Chang et al. 2013). However, it has been noted that the stiffness of the perimeter column has significant effect on modal damping ratios (Tan et al., 2014) .

Inerter devices (Smith, 2002), in many cases, are utilized as a mass amplifier with heavy flywheel, for example, tuned viscous mass damper (Ikago et al. 2012) and tuned inerter damper (Lazar et al. 2013)

[1] Earthquake Engineering Research & Test Center, Guangzhou University, Guangzhou, China, ptan@gzhu.edu.cn
[2] College of Architecture and Civil Engineering, Beijing University of Technology, Beijing, China, liuhaikunlzlg@163.com
[3] Earthquake Engineering Research & Test Center, Guangzhou University, Guangzhou, China, htma@gzhu.edu.cn
[4] College of Architecture and Civil Engineering, Beijing University of Technology, Beijing, China, yanwm@bjut.edu.cn
[5] Earthquake Engineering Research & Test Center, Guangzhou University, Guangzhou, China, zhoufl@cae.cn
[6] Civil Engineering Protection Research Center, Guangzhou University, Guangzhou, China, huanshi@gzhu.edu.cn

become the alternative approach instead of TMD due to the larger mass amplification for inerter. On the other hand, researchers expected to magnify the deformation for effective energy dissipation with smaller inerter, just as the case for the rotational inertial damper (RID) having a ball screw amplifying deformation without the flywheel (Hwang et al. 2007). In this paper, RID will be introduced to participate in energy dissipation for outrigger system. Based on Bernoulli-Euler beam theory and numerical assembly technique (Wu and Chou, 1999), complex dynamic characteristic equation satisfying the boundary conditions is formulated to obtain the pseudo-undamped natural frequencies and modal damping ratios. Furthermore, finite element model for RID outrigger system is developed to solve the response.

2. MODELLING OF OUTRIGGER SYSTEM WITH RID

The basic schematic diagram of rotation inertia damper is shown in Figure 1, in which a linear motion is transformed to rotational movement due to the ball screw. Note that the small linear displacement is amplified so that more energy from the system can be dissipated in the viscous material.

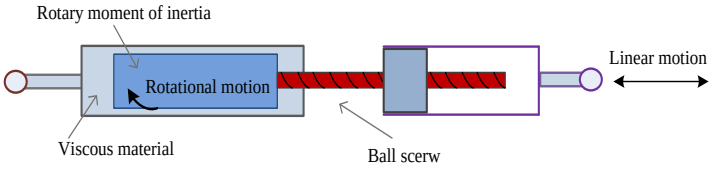

Figure 1. RID model

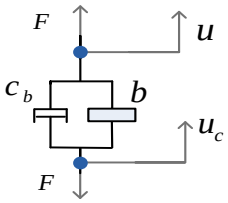

Figure 2. Mechanical model

An RID can be represented by Figure 2 and the force applied can determined using the following expression

$$F = b\left(\ddot{u} - \ddot{u}_c\right) + c_b\left(\dot{u} - \dot{u}_c\right) \tag{1}$$

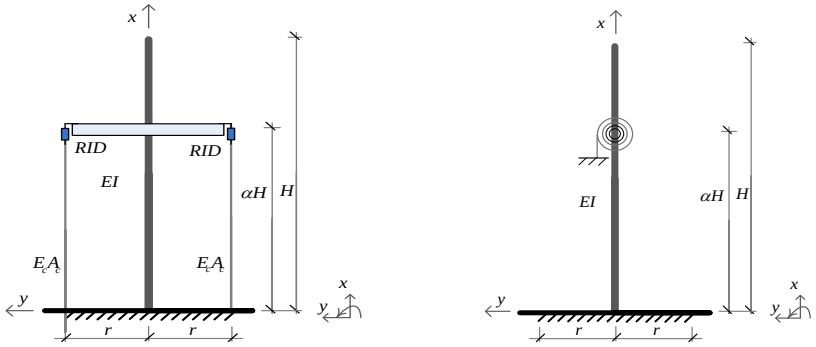

a. Simplified model b. Equivalent model

Figure 3. Models of a high-rise building with RID

where F is the equivalent force caused by RID; b is the nominal mass which is an equivalent

amplified mass because of rotation motion; c_b is the equivalent amplified damping coefficient of the RID; u and u_c are the displacements of the upside and downside of the RID respectively.

Figure 3a presents a simplified model of a high-rise building with RID and Figure 3b shows an equivalent model represented by a rotational spring. It is assumed that the bending rigidity of the outrigger is infinite and the length of each outrigger is r. The bending stiffness of the core is EI and m represents mass for per unit length of the core. E_cA_c is the axial stiffness of the peripheral column, H is the length of the core, and αH is the location of the RID outrigger.
The governing equation of RID can be expressed as:

$$\begin{cases} F_d = b\left(\ddot{u}-\ddot{u}_c\right)+c_b\left(\dot{u}-\dot{u}_c\right) \\ b\left(\ddot{u}_c-\ddot{u}\right)+c_b\left(\dot{u}_c-\dot{u}\right)+k_e u_c = 0 \end{cases} \tag{2}$$

where F_d is the equivalent force caused by RID; $k_e = E_cA_c/(\alpha H)$ represents the axial stiffness of the outer column. With Laplace transform, and considering that $u=\theta r$, the resistant moment of the RID outrigger is

$$M_\theta = -2F_d r = -k_\theta \theta \tag{3}$$

where k_θ is the equivalent resistant rotational stiffness of the RID with the outer column,

$$k_\theta = \frac{2k_e\left(c_b s + bs^2\right)r^2}{k_e + c_b s + bs^2} = \frac{EIk}{H}\left(\frac{2kci - 2k^3\eta^2}{1+2k^2c\alpha\beta i - 2k^4\alpha\beta\eta^2}\right) \tag{4}$$

In which $\eta = \sqrt{\frac{br^2}{mH^3}} = \frac{r}{H}\sqrt{\mu_b}$, $k^4 = \frac{mH^4}{EI}\omega^2$, $s = i\omega$, $c = \frac{c_b r^2}{H\sqrt{mEI}}$, $\beta = \frac{EI}{2E_cA_cr^2}$, $\mu_b = \frac{b}{mH}$. Thus, the equivalent model with a rotational spring shown in Figure 3b can be used to analyze the outrigger system with RID.

3. DYNAMIC CHARACTERISTICS FOR RID OUTRIGGER SYSETM

The motion equation of a vibrating Bernoulli-Euler beam with no damping can be expressed as

$$EI\frac{\partial^4 y(x,t)}{\partial x^4} + m\frac{\partial^2 y(x,t)}{\partial t^2} = 0 \tag{5}$$

where $y(x,t)$ represents the transverse displacement. $y(x,t) = Y(x)e^{i\omega t}$ can be assumed as its solution. Nondimensionalizing Y and x by $\tilde{Y} = Y/H$, $\tilde{x} = x/H$. Considering the situation when only one pair of RID outriggers are used, the cantilever beam is divided into 2 segments. Let the solutions for the segments be expressed as

$$\tilde{Y}_j(\tilde{x}) = F_{j1}\cosh(k\tilde{x}) + F_{j2}\sinh(k\tilde{x}) + F_{j3}\cos(k\tilde{x}) + F_{j4}\sin(k\tilde{x}) \tag{6}$$

where $F_{j\upsilon}$ $(j=1,2;\ \upsilon=1,2,3,4)$ are unknown coefficients for the two segments. The numerical assembly technique (Wu and Chou, 1999) is employed to derive dynamic characteristic equations. With the continuity conditions at the connection point $\tilde{x}=\alpha$, the boundary conditions for the fixed

end of the left of the 1st segment, namely $\tilde{x}=0$ and the boundary conditions for the free end of the right of the 2nd segment $\tilde{x}=1$, one can get the following equation,

$$\mathbf{DF}=\mathbf{0} \tag{7}$$

where **D** is the stiffness parameter and **F** is the unknown coefficient vector. To obtain a nontrivial solution for Equation 7, the determinant of the coefficient matrix must vanish

$$|\mathbf{D}|=0 \tag{8}$$

After rearrangement of Equation 8, one can get

$$\begin{aligned} &k_p[\cos(k-2k\alpha)\sinh(k)+\cosh(k-2k\alpha)\sin(k)+2\cos(k\alpha)\sinh(k\alpha)+2\cosh(k\alpha)\sin(k\alpha)+\\ &\cos(k)\sinh(k)+\cosh(k)\sin(k)-2\cos(k-k\alpha)\sinh(k-k\alpha)-2\cosh(k-k\alpha)\sin(k-k\alpha)]+\\ &4[\cos(k)\cosh(k)+1]=0 \end{aligned} \tag{9}$$

The complex frequency of the RID outrigger system can be expressed as following form

$$i\omega=-\xi\omega_0+i\sqrt{1-\xi^2}\,\omega_0 \tag{10}$$

in which ω_0 is the pseudo-undamped natural circular frequency and ξ is the damping ratio for the system. They are calculated by

$$\xi=-\frac{\mathrm{Re}(i\omega)}{|i\omega|} \tag{11}$$

$$\omega_0=|i\omega| \tag{12}$$

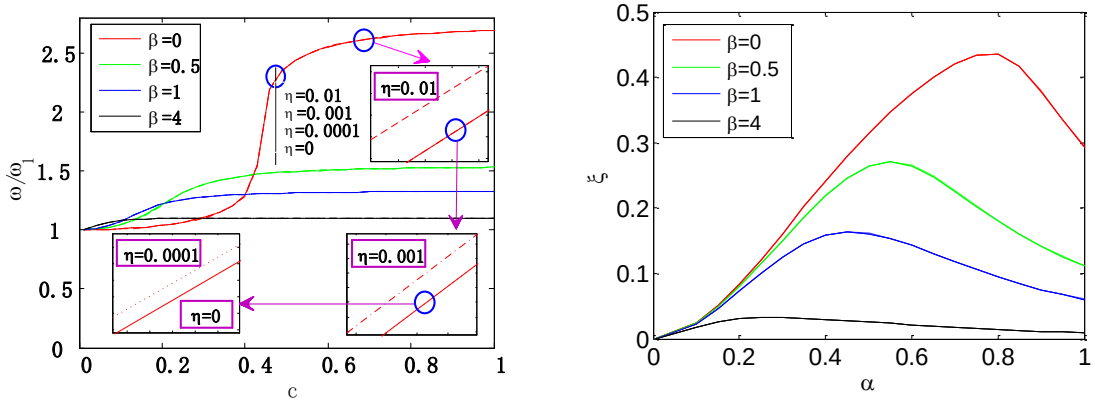

a. First modal frequency ratio versus α b. First modal damping ratio versus α

Figure 4. 1st mode

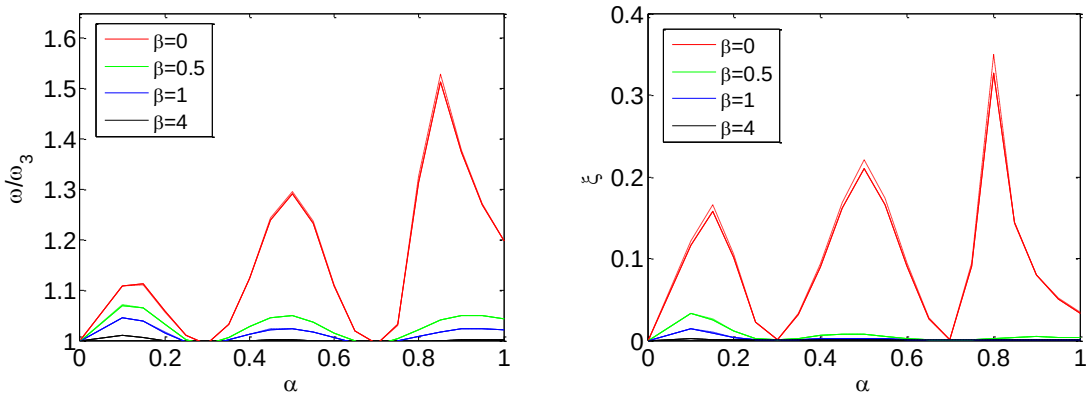

a. Third modal frequency ratio versus α b. Third modal damping ratio versus α

Figure 5. 3rd mode

The pseudo-undamped natural frequency ratios and modal damping ratios versus the position parameter α for RID outrigger with $c = 0.2$ are shown in Figure 4 and Figure 5, in which thumbnails based on the consideration of the space and convenience are plotted for $\beta = 0$ in Figure 4a, but no repetition for $\beta = 0.5,1,4$ and also for Figure 4b and Figure 5. It is interesting that there are one and three peaks for pseudo-undamped natural frequency ratio for different α values for the 1st and the 3rd modes respectively and the similar phenomena can be observed for damping ratios. Obviously, the optimal damping ratio may be achieved at one position for certain mode while bad results may account for the other modes at the same position by analysis of the Figures 4b and 5b. Viewed form Figure 4a, pseudo-undamped natural frequency ratio for the 1st mode increase with α ranging from 0 to 1. It can be found that frequency ratio can reach a relatively higher value for $\beta = 0$ with $\alpha \to 1$, whereas $\beta = 0.5,1,4$, can get their lower maximum in different peaks. It also can be observed that the curves for $\beta = 0$ under different mass parameters such as $\eta = 0$, $\eta = 0.0001$, $\eta = 0.001$, $\eta = 0.01$ always coincide, as well as the same cases for $\beta = 0.5$, $\beta = 1$, $\beta = 4$ in Figure 4a and also for Figure 4b and Figure 5. These phenomena demonstrates that mass parameters η hardly play a role on the frequency ratios and damping ratios varying versus position for of the RID outrigger whereas stiffness parameter has significant influence on them.

4. CASE STUDY

To determine the response of the outrigger structure with RID under seismic excitations, finite-element (FE) method is utilized. Let the RID outrigger is installed at node j. The displacement u_c in the RID is added to the displacement vector and the displacement components at node j will be u_j, θ_j, u_c. Thus, the displacement vector to be considered will be

$$\boldsymbol{u}_f = \{u_1, \theta_1, \cdots, u_{j-1}, \theta_{j-1}, u_j, \theta_j, u_c, u_{j+1}, \theta_{j+1}, \cdots, u_n, \theta_n\} \tag{13}$$

After beam elements have been assembled, one can obtain the dynamic equation for the whole system

$$\boldsymbol{M}_f \ddot{\boldsymbol{u}}_f + \boldsymbol{C}_f \dot{\boldsymbol{u}}_f + \boldsymbol{K}_f \boldsymbol{u}_f = \boldsymbol{\Gamma} \ddot{u}_g \tag{14}$$

where $\boldsymbol{M}_f, \boldsymbol{C}_f, \boldsymbol{K}_f$ are the global mass matrix, global damping matrix and global stiffness matrix, and $\boldsymbol{\Gamma} \ddot{u}_g$ is the earthquake action vector in which the location for RID outrigger is set to be 0.

A numerical example for RID outrigger system is provided to investigate its parameters and performance of the seismic mitigation. The main model parameters are as follows: $EI = 1.47\times10^{13}\ Nm^2$, $m = 1.08\times10^5\ kg/m$, $H = 200\ m$, $r = 15\ m$, $\xi_0 = 0.02$. Also, two typical seismic records are applied to investigate the performance of the RID outrigger system. They are for the NS component of 1940 El Centro earthquake and Kobe earthquake in 1995, both of which are adjusted to the maximum ground acceleration of 3m/s2.

Table 1 Mass parameters

η	μ_b	b **(kg)**
0.002	0.0007	1.54×10^4
0.01	0.0178	3.84×10^5
0.1	1.78	3.84×10^7

Mass information of RID can be deduced in Table 1 with the determined η. From Table 1, one can observe that $\eta = 0.1$ may not be practical because the corresponding nominal mass ratio (μ_b) of RID is far too big. It is also not quite reasonable for $\eta = 0.01$ with the reason that the nominal mass $b = 3.84\times10^5\ kg$ of RID means hundreds of times than its real physical mass of which is generally several tons. Commonly, it is not necessary for RID using flywheel to create the large inertia force (amplified mass), contrarily, the amplified mass for RID should be designed to be much smaller, for instance several times or ten times. However, $\eta = 0.002$ with the nominal mass $b = 1.54\times10^4\ kg$ is suitable for RID with several tons of physical mass.

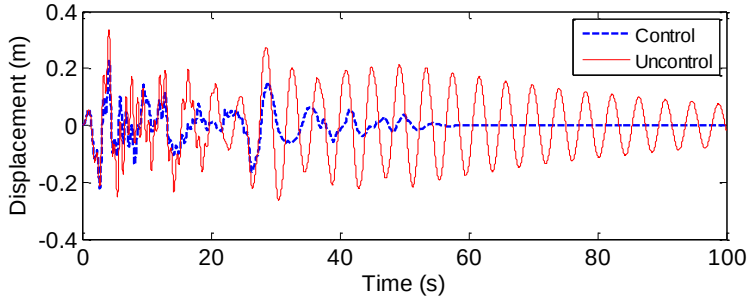

a. Displacement

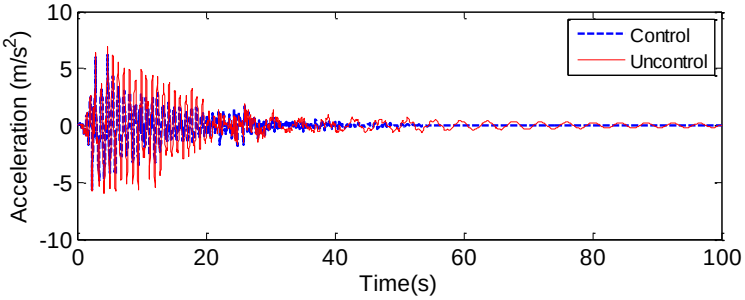

b. Absolute acceleration

Figure 6. Response under El Centro excitation

The responses at the top of the structure under the earthquake excitations for $c = 0.2$, $\beta = 0.5$, $\eta = 0.002$, $\alpha = 0.68$ are shown in Figures 6 (Response under Kobe record no presenting). The numerical simulation results show that the structure with RID outriggers have excellent control

performance for the displacement and the acceleration. Reductions in peak responses are 69.23 % in displacement and 80.54 % in acceleration for Kobe wave, and 67.59% in displacement and 90.20 % in acceleration for El Centro wave. Obvious, the results indicate that the use of RID is effective for vibration suppressing.

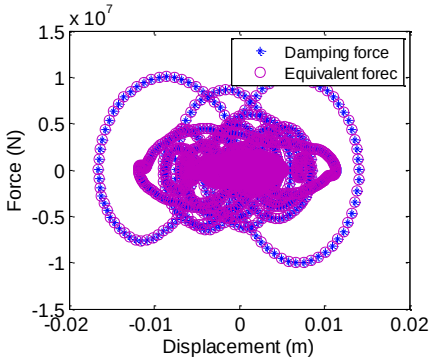

a $\eta = 0.002$

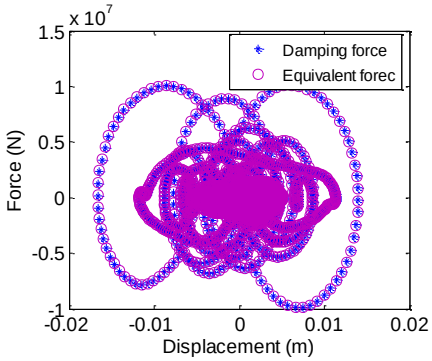

b. $\eta = 0.01$

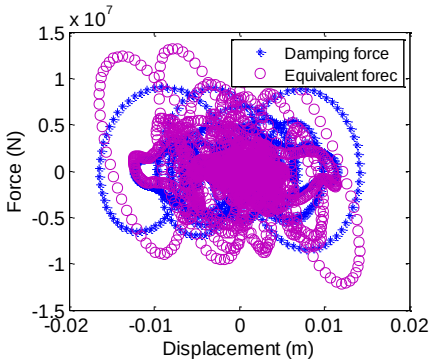

c. $\eta = 0.1$

Figure 7. Force-deformation under El Centro excitation

Figure 7 presents the force-displacement relationship of the structure with RID outriggers subjected to El Centro excitation. Curves for the total equivalent force of RID and just damping force are included. Note that the total equivalent force includes both damping force and inertia force caused by RID. It can be easily found that, for the two case of $\eta = 0.002$ and $\eta = 0.01$, the damping force of RID is predominant and the inertia force is negligible. For the third case, where the RID has an excessively large mass, histories of the total equivalent force of RID and damping force are significantly different, indicating that inertia force of RID is important for this unpractical case.

5. CONCLUSIONS

The rotation inertia damper was introduced to outrigger system to suppress excessive vibrations of high-rise buildings. Based on Bernoulli-Euler beam theory, an equivalent analysis model was proposed to simulate the structure with RID outrigger. The numerical results show that RID outrigger system has an excellent control performance. The relative bending stiffness of the peripheral columns has a significant influence on the pseudo-undamped natural frequency ratios and modal damping ratios of the structure, while the mass parameter of RID has little effect. Moreover, the damping force in RID is predominant and the inertia force is insignificant.

6. ACKNOWLEDGMENTS

This work was supported by the Program for Changjiang Scholars and Innovative Research Team in University (Grant No. IRT13057) and the National Natural Science Foundation of China (Grant No. 51478129,51408142), and also in part by Guangdong Special Program (Grant No. 2014TX01C141) and Yangcheng Scholars Program (Grant No. 1201541630)

7. REFERENCES

Chang CM, Wang Z, Spencer BF, Chen Z (2013). Semi-active damped outriggers for seismic protection of high-rise buildings. *Smart Structures & Systems*, 11(5): 435-451.

Chen Y, Mcfarland DM, Wang Z, Spencer BF, Bergman LA (2010). Analysis of Tall Buildings with Damped Outriggers. *Journal of Structural Engineering*, 136(11): 1435-1443.

Hwang JS, Kim J, Kim YM (2007). Rotational inertia dampers with toggle bracing for vibration control of a building structure. *Engineering Structures*, 29(6): 1201-1208.

Ikago K, Saito K, Inoue N (2012). Seismic control of single-degree-of-freedom structure using tuned viscous mass damper. *Earthquake Engineering & Structural Dynamics*, 41(3): 453–474.

Lazar IF, Neild SA, Wagg DJ (2013). Using an inerter-based device for structural vibration suppression. *Earthquake Engineering & Structural Dynamics*, 43(8): 1129–1147.

Satake N, Suda K, Arakawa T, Sasaki A, Tamura Y (2003). Damping Evaluation Using Full-Scale Data of Buildings in Japan. *Journal of Structural Engineering*, 129(4): 470-477.

Smith MC (2002). Synthesis of mechanical networks: the inerter. *IEEE Transactions on Automatic Control*, 47(10): 1648-1662.

Smith RJ, Willford MR (2007). The damped outrigger concept for tall buildings. *Structural Design of Tall & Special Buildings*, 16(4): 501-517.

Tan P, Fang CJ, Zhou F (2014). Dynamic characteristics of a novel damped outrigger system, Earthquake Engineering and Engineering Vibration, 13(2) 293-304.

Willford M, Smith R, Scott D, Jackson M (2008). Viscous Dampers Come of Age. *Structure Magazine*, 6: 15-18

Wu JS, Chou HM (1999). A new approach for determining the natural frequency and mode shapes of a uniform beam carrying any number of sprung masses. *Journal of Sound & Vibration*, 220(3): 451-468.